### **Effect of Polymer Concentration on Autoclaved Cryogel Properties**

Adnan Memic, Mahboobeh Rezaeeyazdi, Pierre Villard, Zachary J. Rogers, Tuerdimaimaiti Abudula, Thibault Colombani, Sidi A. Bencherif\*

Prof. Adnan Memic, Pierre Villard, Dr. Tuerdimaimaiti Abudula Center of Nanotechnology, King Abdulaziz University, Jeddah, Saudi Arabia

Pierre Villard, Zachary J. Rogers, Dr. Thibault Colombani and Prof. Sidi A. Bencherif Department of Chemical Engineering, Northeastern University, Boston, USA

Prof. Sidi A. Bencherif

Department of Bioengineering, Northeastern University, Boston, USA; Harvard John A. Paulson School of Engineering and Applied Sciences, Harvard University, Cambridge, MA, USA; Sorbonne University, UTC CNRS UMR 7338, Biomechanics and Bioengineering (BMBI), University of Technology of Compiègne, Compiègne, France,

E-mail: s.bencherif@northeastern.edu

Keywords: Autoclave Sterilization, Biopolymers, Physical Properties, Cryogels, Biomedical Applications

Biomaterial sterilization is a prerequisite prior to patient's use, especially for scaffold implantation or injection. Various sterilization processes are mandated by the Food and Drug Administration including high-pressure steam sterilization. Although high-pressure steam or autoclave sterilization eliminates pathogens, it often leads to irreversible damages of soft materials such as hydrogels. In the current study, the impact of autoclave sterilization on cryogels made from several naturally-derived polymeric precursors (alginate, hyaluronic acid, and gelatin) is analyzed. Specifically, the impact of polymer concentration on the structural and physical properties of autoclaved cryogels such as mechanics, swelling ratio, pore interconnectivity, and shape-memory features is studied. The results demonstrate that at an optimal polymer concentration, independent of the biopolymer investigated, autoclave sterilization does not substantially alter the microarchitectural and physical characteristics of cryogels, including their syringe injectability signature. In summary, when formulated under

optimized conditions, autoclavable cryogels hold great potential for several biomedical applications, as they can be easily translated into clinical practice to benefit public health.

### 1. Introduction

During the past several decades, polymeric biomaterials have attracted a lot of interest from researchers in various fields, especially those working in bioengineering.<sup>[1-3]</sup> Specifically, biomaterials have the potential to play a critical role in biosensing, drug delivery, immunotherapy and tissue engineering.<sup>[4-6]</sup> For example, they could be used to repair or replace damaged parts of living systems or diagnose first instances of disease.<sup>[7-9]</sup> However, their recent use as surgical implants has led to a number of healthcare-associated infections. <sup>[10]</sup> Therefore, it is vital for biomaterials to be fully sterile in a clinical setting to keep patients safe.<sup>[11,12]</sup>

In medical device manufacturing, sterilization is any process that kills, deactivates, or eliminates all know pathogens and biological agents and is therefore critical for patient safety. [12-14] Sterilization can be achieved using several techniques including irradiation, filtration, chemical addition, heat, and high pressure treatment. However, many of these methods have challenges that prevents their widespread application for biomaterial sterilization. [12, 14, 15] For example, scaffolds made from naturally-derived polymers are often degraded when gamma-ray irradiation is applied. [16] To mitigate degradation, researchers have turned to other approaches such as ethylene oxide (EtO) gas. However, EtO treatment often leads to residual vapor toxicity, limiting its use by the biomedical industry. [17, 18] Furthermore, many sterilization methods are costly and often inaccessible, forcing many research laboratories to resort to less rigorous methods during their studies like disinfection including ethanol treatment. [19] Although ethanol has little to no negative effects on most biomaterial properties, it is unable to inactivate bacterial spores, making this method insufficient for clinical translation. [20-22] High-pressure steam sterilization, or autoclaving, is one of the most popular

sterilization methods, due to its capacity to eliminate all types of pathogenic organisms.<sup>[23, 24]</sup> However, because this method uses highly pressurized steam that has been heated up to 134°C, it is detrimental to several types of biomaterials, including polymeric hydrogels.<sup>[12, 25]</sup>

Cryogels, an advanced class of hydrogels, obtain their unique, improved properties from their fabrication process, cryopolymerization (i.e, free radical polymerization of natural and synthetic monomers or polymers at subzero temperatures). [26-28] During cryopolymerization, ice crystals form, concentrating the polymer into an unfrozen phase in which crosslinking occurs. When the gels are brought to room temperature (RT), the ice crystals thaw, leaving behind an interconnected, macroporous structure surrounded by dense polymer walls. Cryogels display superior mechanical and physical properties compared to their conventional (i.e., nanoporous) hydrogel counterparts. Furthermore, cryogels are reversibly collapsible and exhibit shapememory properties, allowing them to be injected through a standard small-bore needle. [28] Due to their unique properties, cryogels have been used in several biomedical applications, including drug delivery, cancer immunotherapy and tissue engineering. [26, 29-31] We hypothesized that cryogels, which have improved properties and hydrolytic stability compared to conventional hydrogels, would be resistant to autoclave-induced degradation and thus easily translatable into the clinic.

Currently, cryogels are typically not sterilized but rather sanitized, especially in academic institutions. Nevertheless, translating cryogel scaffolds into a clinical setting for patients' use would necessitate terminal sterilization. To this end, we have recently developed mechanically robust injectable cryogels that remain unchanged after autoclaving. [25, 32-35] However, the effect of polymer concentration, the driving force for gel formation, on the properties of autoclaved cryogels has not been investigated. Therefore, in this study, we prepared a series of cryogels made from various biopolymers at different polymer concentrations. [36, 37] Next, we assessed how the polymer concentration can impact the physical properties and integrity of autoclaved

cryogels as well as their syringe injectability. This work reports that, unlike conventional hydrogels, injectable cryogels can be resilient to the aggressive steam sterilization conditions when formulated at optimal polymer concentrations. These unique and advanced properties could extend applications of cryogels in the broader biomedical arena and further push their translatability into the clinic.

#### 2. Results

### 2.1. Characterization of Modified Polymers and Cryogel Fabrication

In our study, cryogels were fabricated by first grafting pendant methacrylate residues along the backbone of various naturally-derived polymers (Figure 1). Specifically, we methacrylated three biopolymers, namely, hyaluronic acid (HAGM), alginate (MA-Alginate), and gelatin (MA-Gelatin). Subsequently, these biopolymers were crosslinked at T< -20 °C to form cryogels. In Figure 2, changes in the molecular structure of each biopolymer upon chemical modification and their subsequent cryogelation in water are depicted. The synthesis of HAGM was based on the reaction of HA with glycidyl methacrylate (GM). During this process, GM reacts primarily with HA via an irreversible ring-opening reaction with HA's carboxylic acid groups toward the highest substituted carbon of GM's epoxides. Similarly, MA-Alginate was synthesized through the conjugation of amine-terminated AEMA with alginate's activated carboxylic acid groups. Finally, MA-Gelatin was prepared by reacting methacrylic anhydride (MA) with gelatin, resulting in the grafting of methacrylate residues along the polymer backbone (Figure 2). <sup>1</sup>H NMR spectroscopy was used to confirm polymer modification as depicted by the vinyl methylene peaks ranging between 5.5 and 7.0 ppm for HAGM, 5.0 and 6.0 ppm for MA-Alginate, and 5.5 and 7.0 ppm for MA-Gelatin. Degrees of polymer methacrylation were found to be 31%, 34%, and 25% for HAGM, MA-Alginate, and MA-Gelatin, respectively. Additionally, <sup>1</sup>H NMR was also used to evaluate the consumption of vinylic groups following cryogel fabrication. As shown in Figure 2 (inset spectra), the



disappearance of vinyl methylene groups suggest that high vinyl conversions can be achieved for all three types of cryogels regardless of their polymer concentrations.

### 2.2 Evaluating Pore Size and Macroporous Structural Features

One main advantage of cryogels is their inherent microstructural features. As shown in **Figure 3**, cryogels across the different polymer concentrations and type display an interconnected porous network with pores surrounded by densely packed polymer walls. We observed minimal changes in terms of pore size following autoclaving. For instance, 2%, 4%, and 6% w/v HAGM cryogels exhibit an average pore size of 70, 50, and 30 µm pre-autoclave and 60, 45, and 30 µm post-autoclave treatments, respectively (**Figure 3A**). Similarly, for 1% and 2% w/v MA-Alginate cryogels, average pore sizes also remain unchanged, estimated to be 60 and 30 µm pre-autoclave and 60 and 35 µm post-autoclave treatments, respectively (**Figure 3B**). MA-Gelatin cryogels also displayed resilience to steam sterilization. The average pore sizes for 5%, 8%, and 10% w/v MA-Gelatin cryogels were estimated to be 55, 40, and 30 µm pre-autoclave and 60, 35, and 30 µm post-autoclave treatments, respectively (**Figure 3C**). Additionally, SEM images suggest that the network structure and pore morphology remained unaltered through the process of autoclaving across all three biopolymers tested at various concentrations. It should also be noted that cryogels formulated at higher polymer concentrations exhibit thicker polymer walls and smaller pore sizes.

### 2.3 Characterizing the Physical Properties of Cryogels

We evaluated the effect of polymer concentration on the physical properties (i.e., mechanics, swelling ratio, and pore interconnectivity) of HAGM, MA-Alginate, and MA-Gelatin cryogels. Their corresponding (nanoporous) hydrogels prepared from the same polymer formulations were also tested as control groups (**Figures 4, 5,** and **6**). As expected, conventional hydrogels deteriorated upon autoclave sterilization.<sup>[38, 39]</sup> These samples were challenging to characterize

as they were either partially or fully degraded (i.e., liquified) following autoclave treatment. For instance, 2% w/v HAGM conventional hydrogels entirely degraded after autoclaving, resulting in a gel-to-sol transition most likely due to polymer break down via hydrolysis (**Figure 4**). Similarly, 1 and 2% w/v MA-Alginate, and 5 and 8% w/v MA-Gelatin hydrogels did not sustain autoclaving and no data could be recorded (**Figures 5** and **6**). On the other hand, for the partially degraded hydrogels (4 and 6% HAGM, 10% MA-Gelatin), these gels exhibited lower Youngs' moduli and higher swelling ratios post-autoclave treatment. In general, across the three investigated biopolymers and at a given polymer concentration, non-autoclaved hydrogels exhibited higher mechanical stiffnesses and lower pore interconnectivities when compared to their cryogel counterparts.

We also examined the effect of polymer concentration on the physical properties of cryogels across the three biopolymers. For HAGM, increasing the polymer concentration from 2 to 6 % w/v resulted in cryogels with higher young's moduli, ranging from ~3kPa to ~10kPa, and a slight decrease in their swelling ratios, ranging from ~40 to ~38 (Figure 4). Strikingly, autoclave treatment did not significantly alter their physical characteristics (mechanics and swelling ratios), except at the lower concentration tested. Surprisingly, HAGM cryogels' high degrees of pore interconnectivity (≥ 80%) remained unchanged regardless of the polymer concentration and autoclave treatment. For MA-Alginate, increasing the polymer concentration from 1 to 2 % w/v resulted in cryogels with a notable increase in their Young's moduli, from ~4kPa to ~6kPa, and a slight increase in their swelling ratios, from ~45 to ~50 (Figure 5). Unlike HAGM cryogels, autoclave treatment seemed to slightly alter the physical characteristics of MA-Alginate cryogels—Young's moduli moderately decreased while the swelling ratios increased. However, their degrees of pore interconnectivity (> 80%) remained comparable. It is important to note that unlike cryogels, all MA-Alginate hydrogels entirely degraded post-autoclaving. For MA-Gelatin, increasing the polymer concentration from 5 to 10

% w/v resulted in cryogels with higher Young's moduli, ranging from ~5kPa to ~18kPa, and a slight decrease in their swelling ratios, ranging from ~20 to ~18 (**Figure 6**). The autoclave treatment slightly impacted their physical characteristics—Young's moduli moderately decreased while the swelling ratios either increased or remained alike. However, their degrees of pore interconnectivity (> 75%) remained nearly the same.

### 2.4 Testing Cryogel Syringeability and Injectability

To assess the effect of polymer concentration and autoclave treatment on cryogel injectability, cuboid-shaped cryogels (dimensions: 4 mm x 4 mm x 1 mm) were suspended in PBS and syringe-injected by means of a 16-gauge needle. As shown in **Figure 7**, rhodamine-labeled HAGM (4 % w/v), MA-Alginate (2% w/v), and MA-Gelatin (10% w/v) cryogels were able to be successfully injected without any visual damages (i.e., gel fragmentation). More strikingly, these cryogels overcame autoclave sterilization, remained syringe-injectable, and retained their inherent shape-memory features. On the other hand, other cryogels (MA-Alginate: 1%, HAGM: 2 and 6%, MA-Gelatin: 5 and 8% w/v) were not injectable neither before nor after. This is likely due to their poor physical properties (MA-Alginate: 1%, HAGM: 2%, MA-Gelatin: 5 and 8% w/v) or brittleness (i.e., stiff cryogels) as a result of dense and thick polymer walls at high polymer concentrations (HAGM: 6% w/v).

#### 3. Discussion

There is an increasing need to engineer advanced and enduring biomaterials for clinical use. One of the major challenges with translating polymeric scaffolds from bench to bed side is ensuring their complete sterilization prior to delivery into the body. When sterilizing biodegradable scaffolds, the chosen sterilization technique must maintain their structural integrity, thereby ensuring they can fulfill their intended purposes post-sterilization.<sup>[18]</sup> We recently reported that cryogels are the first type of polymeric gel scaffold that can sustain

autoclave sterilization, a gold standard for sterilizing biomedical devices.<sup>[25]</sup> To this end, we aimed to better understand the effect of polymer concentration on the physical properties of cryogels before and after autoclave sterilization. Therefore, we developed these injectable and autoclavable cryogels using three different methacrylated biopolymeric precursors. We observed that all cryogels had a different optimal polymer concentration that would allow them to be injected pre- and post-steam sterilization. Although cryogels were fabricated at low polymer concentrations (unlike their conventional hydrogel counterparts which remain in a solution form) and sustain autoclave sterilization, they ultimately yielded non-injectable and mechanically weak cryogels. Their inadequate physical integrity is more likely due to low crosslink densities, thereby leading to weak mechanical strength.<sup>[33]</sup> Alternatively, having a higher polymer content leads to the fabrication of stiffer and brittle gels that is most likely a result of thick and dense polymer walls. Therefore, cryogels with too low or too high polymer content are susceptible to fracture and damage during injection. However, cryogels with optimum polymer content (i.e., 2% MA-Alginate, 4% HAGM, and 10% MA-Gelatin) can withstand injection-associated shear stress while remaining resilient to autoclave treatment.

Cryogels that remained physically weak would require further investigation of different approaches to improve their physical properties. Several strategies could be applied to achieve this effect including increasing the crosslinker density or the methacrylation degree during the chemical modification of polymers. [30, 32, 40, 41] However, when augmenting the methacrylation degree of polymers, it is important to ensure complete vinyl methylene consumption following cryopolymerization as depicted in **Figure 2**. This observation is critical as any residual unreacted groups could cause significant toxicity once introduced in the body. [33, 42] Alternatively, it might be necessary to develop other cryogel fabrication approaches or chemistries. [25, 30, 33, 43] However, it is hypothesized that only covalent crosslinking strategies will yield autoclavable, mechanically stable and robust cryogels. Previously reported examples

of physically crosslinked<sup>[44]</sup> cryogels did not provide adequate mechanical properties to overcome shear and sterilization associated damages.

We hypothesize that cryogel's unique features including their highly crosslinked and dense polymer walls in combination to an open macroporous network provide the required hydrolytic and mechanical stability prior- and post-autoclave treatment. [3, 32, 45] These superior properties make autoclavable cryogels much more attractive than their conventional hydrogel counterparts, especially as scaffolds for tissue engineering applications. [2, 3, 46] Additionally, the comparison of conventional hydrogels to their cryogel counterparts revealed significant differences in terms of swelling ratio and pore interconnectivity changes during autoclave sterilization. Conventional hydrogels exhibited very low initial pore interconnectivity and large swelling ratio increase after autoclave sterilization. However, cryogels remained stable most likely due the nature of their highly crosslinked and dense polymer walls.<sup>[45, 47]</sup> We anticipate that these tunable properties could be used to better recapitulate the microenvironmental niche of tissues by promoting cell-material interactions as well as cell infiltration and trafficking. Further, these characteristics could emulate native soft tissue mechanics and support the exchange of nutrients, oxygen, and waste. [30, 48-50] Similarly, it might be important to take into account these traits when developing newly emerging bioinks, dermal fillers and immunotherapeutic scaffolds. [29, 34, 51-57]

Although we formulated several cryogels using three different biopolymers and concentrations, we did not characterize in-depth their associated biological properties in this report. Further studies are needed to better understand the relationship between the physical and biological properties of these cryogels. Specifically, it would be important to optimize the biodegradation profiles of these cryogels. Similarly, it is important to study the long-term *in-vivo* biocompatibility of cell-laden cryogel as a continuation of our existing work. [25] Further studies might also include synthetic polymeric precursors for the development of mechanically

and hydrolytically stable cryogels. Finally, although we show injection of cryogels that were 16mm<sup>3</sup> large, in some cases it may be essential to inject bigger cryogels. We anticipate that hybrid or nanocomposite cryogel formulations will be able to go beyond the current limit of 64mm.<sup>3</sup> [35] However, in such cases where larger cryogels are required, they can potentially be injected through a catheter to permit their minimally invasive delivery in the body.

#### 4. Conclusion

In summary, we have described for the first time how the polymer concentration can impact the physical properties of cryogels both before and after autoclave treatment. Similarly, we compared how cryogels are superior relative to their conventional hydrogel counterparts. We show that the polymer concentration can be adjusted and optimized to engineer cryogels with robust and improved mechanical properties, independent of the type of polymer studied. Unlike hydrogels, the macroporous, highly dense and interconnected polymer network at suitable polymer concentrations (i.e., 2% MA-Alginate, 4% HAGM, and 10% MA-Gelatin) make cryogels more resistant to hydrolytic degradation. We further demonstrated that following autoclave sterilization no significant changes occur to their overall structural features, including pore morphology and interconnectivity. Finally, these optimized cryogels are shown to be mechanically resilient. As a result, they overcome shear-stress and exhibit excellent injectability both pre- and post-autoclave treatment. Collectively, all these advantageous features make these autoclavable and syringe-injectable cryogels great candidates as polymeric scaffolds for a wide range of biomedical applications, including biosensing, drug delivery, immunotherapy and tissue engineering.

### 5. Experimental Section

Methacrylate groups were introduced into the biopolymers used in this study to make them amenable to free radical polymerization, crosslinking, and ultimately gelation. [25, 28, 32]

Synthesis of Methacrylated Hyaluronic Acid (HAGM). Methacrylate groups were conjugated to the sodium salt of hyaluronic acid (HA) to prepare HAGM. A total of 1.0 g of HA (Sigma-Aldrich) was dissolved in 200 mL phosphate buffered saline (pH 7.4, PBS, Sigma-Aldrich). Next, 67 mL of dimethylformamide (Sigma-Aldrich), 13.3 g of glycidyl methacrylate (GM, Sigma-Aldrich), and 6.7 g of triethylamine (Sigma-Aldrich) were then added sequentially to the hyaluronic acid solution. Following 10 days reaction at RT, the solution was then precipitated in an excess of acetone, filtered, dried in vacuum oven overnight, and finally stored at -20 °C until further use.

Synthesis of Methacrylated Alginate (MA-Alginate). A total of 1.0 g of sodium alginate (Sigma-Aldrich) was dissolved in 100 mM of 2-(N-morpholino)ethanesulfonic acid buffer (0.6% w/v, pH 6.5, MES, Sigma-Aldrich). Once sodium alginate was fully dissolved, 1.3 g of N-Hydroxysuccinimide (NHS, Sigma-Aldrich) and 2.8 of 1-Ethyl-3-(3g dimethylaminopropyl)carbodiimide (EDC, Sigma-Aldrich) were added to the mixture to activate the carboxylic acid moieties along the alginate backbone. Next, 2.24 g of 2-aminoethyl methacrylate hydrochloride (AEMA, Sigma-Aldrich) was added to the mixture (molar ratio of NHS:EDC:AEMA = 1:1.3:1.1). After an overnight reaction at RT, the product was precipitated in an excess of acetone, filtered, dried in a vacuum oven overnight, and finally stored at -20 °C until further use.

Synthesis of Methacrylated Gelatin (MA-Gelatin). A total of 8 g of type-A gelatin from porcine skin (Sigma-Aldrich) was dissolved in deionized water (d-H<sub>2</sub>O) while stirring at 60 °C. Subsequently, 50 ml of dimethyl sulfoxide (DMSO, Sigma-Aldrich), a 60-fold molar excess of methacrylic anhydride (Sigma-Aldrich), and 3 g of triethylamine (Sigma-Aldrich) were added to the solution.<sup>2</sup> After 3 days of chemical reaction at 60 °C, the modified polymer was precipitated in an excess of cold methanol, filtered, dried in a vacuum oven overnight at RT, and then stored at -20 °C until further use.

Synthesis of Rhodamine-conjugated Bovine Serum Albumin. NHS-Rhodamine was added to sodium bicarbonate buffer containing bovine serum albumin (BSA, Sigma-Aldrich, 1% w/v (pH 8.5). The reaction proceeded for 4 h in sodium bicarbonate buffer (pH 8.5) at RT and the solution was subsequently freeze-dried to obtain Rhodamine-conjugated BSA.

Hydrogel and cryogel fabrication. Hydrogel and cryogels were fabricated via a redox-induced free-radical polymerization process in water at RT and -20 °C, respectively.<sup>3</sup> For cryogel fabrication, the modified polymers were individually dissolved in d-H<sub>2</sub>O to the desired final concentration with the addition of 0.1% w/v tetramethylethylenediamine (TEMED, Sigma-Aldrich) and 0.4% w/v ammonium persulfate (APS, Sigma-Aldrich). Rhodamine-conjugated BSA was also added to the polymer solutions in order to make them more visible during injection. The prepolymer solutions were pre-cooled at 4 °C before pouring into Teflon molds with desired shape and dimensions, transferred to a freezer to -20 °C temperature, allowing cryopolymerization. After 15 h of chemical reaction, the resulting cryogels were brought to RT and washed with d-H<sub>2</sub>O. The conventional hydrogels used in this study were fabricated from the same prepolymer solutions containing 0.8% w/v APS and 0.2% w/v TEMED through redoxinduced free-radical polymerization in d-H<sub>2</sub>O at RT.

Chemical Characterization of Polymers and Cryogels by <sup>1</sup>H NMR. To calculate the degree of methacrylation and also assess vinyl group consumption, <sup>1</sup>H nuclear magnetic resonance (NMR) spectroscopy analysis was performed following cryopolymerization/gelation using an Inova-500 NMR spectrometer (Varian Medical Systems, Palo Alto, CA, USA). The solvent used was deuterium oxide (D<sub>2</sub>O) while the modified polymer concentration was kept at 2% w/v for HAGM, 1% w/v for MA-Alginate, and 5% w/v MA-Gelatin. For chemical characterization of the cryogels, cylinder cryogels (6 mm diameter, 6 mm height) were freeze-dried, crushed to a fine powder and dispersed in D<sub>2</sub>O. All <sup>1</sup>H NMR spectra were obtained at RT, 15 Hz sample spinning, a 10 s recycle delay, for 128 scans at a 45° tip angle for the observation pulse. Peak

values at 5.4 and 5.7 ppm for MA-gelatin, at 5.15 and 5.3 ppm for MA-Alginate, and at 5.2 and 5.5 ppm for HAGM were correlated to the presence of methacrylated (MA) groups. Peak areas were integrated using ACD/Spectrus NMR analysis software and for each polymer type the degree of methacrylation was determined.<sup>1–3</sup>

Autoclave Sterilization of Hydrogels and Cryogels. For autoclave sterilization, fabricated hydrogels and cryogels were first placed in glass beakers containing d-H<sub>2</sub>O and subsequently sterilized on a liquid cycle for 40 min at 120 °C and 100 kPa in a laboratory autoclave (Tuttnauer, Hauppauge, NY, USA). After autoclaving, samples were rinsed three times in sterile d-H<sub>2</sub>O and then stored at 4 °C until further use.

Mechanical Testing. Young's moduli of cylindrical hydrogel and cryogels (6-mm diameter, 6-mm height) before and after autoclave sterilization were determined using an Instron 5944 testing system (Instron, Norwood, MA, USA). The samples were dynamically deformed (i.e., at a constant rate) between two parallel plates for 10 cycles with a strain rate of 10% per minute. The load (N) and compressive strain (mm) were measured at the 8<sup>th</sup> cycle utilizing Instron's Bluehill 3 software. To determine the moduli, we acquired the tangent of the slope of the linear region on the loading stress/strain curve. Throughout the tests the gel cylinders were kept hydrated in PBS (pH 7.4).

Swelling Measurements. The swelling ratios were measured by a conventional gravimetric procedure. To characterize the swelling ratios, cylindrical hydrogels and cryogels (6-mm diameter, 6-mm height) were fabricated and submersed in PBS for 24 h prior to testing. The equilibrium mass swelling ratio (Q<sub>M</sub>) was calculated by dividing the mass of fully swollen samples by the mass of freeze-dried ones.

Determination of Pore Interconnectivity. The pore interconnectivity was evaluated using a water-wicking technique in which the interconnected porosity was calculated as the

interconnected void volume over the total volume. Fully hydrated hydrogels and cryogels (17-mm diameter, 1-mm thickness) were first weighed on an analytical scale. Kimwipes were used to wick away free solvent (i.e., water) within interconnected pores, and the gels were weighed once again. The degree of pore interconnectivity was then calculated by dividing the mass difference between the fully swollen and partially dehydrated samples to the mass of the fully swollen ones.

Testing Syringe Injectability. The effects of polymer concentration and autoclave treatment were investigated on cryogel injectability. Cuboid-shaped cryogels (4-mm x 4-mm x 1-mm) were first fabricated and subsequently suspended in 0.2 mL of PBS. Next, these cryogels were syringe-injected using a 16-gauge needle. Briefly, cryogels were placed on the needle aperture and injected.

Scanning Electron Microscopy (SEM) Imaging. SEM was used to assess the highly macroporous network of cryogels before and after autoclave treatment across various biopolymers and polymer concentrations. Cryogel samples were first freeze-dried. Next cryogel samples were adhered onto sample stubs using carbon tape and subsequently coated with platinum in a sputter coater. Finally, to image the cryogel samples, secondary electron detection operating at 5 kV and 10 μA was used on a Hitachi S-4800 scanning electron microscope (Hitachi High-Technology Corporation, Tokyo, Japan).

Statistical Analyses. Data are shown as mean  $\pm$  standard deviations (SD). To determine significant statistical differences the Bonferroni post-test and the one- or two-way analysis of variance (ANOVA) test were used. Statistically significant difference of p< 0.05 was accepted and indicated in the figures as \*p< 0.05, \*\*p< 0.01, and \*\*\*p< 0.001.

Abbreviations. RT, room temperature; SD, standard deviation; 3D, three-dimensional; ANOVA, analysis of variance; SEM, scanning electron microscopy; NMR, nuclear magnetic

resonance; DMSO, dimethyl sulfoxide; BSA, bovine serum albumin; EDC, 1-Ethyl-3-(3-

dimethylaminopropyl)carbodiimide; NHS, N-Hydroxysuccinimide; AEMA, 2-aminoethyl

methacrylate hydrochloride; PBS, phosphate buffered saline; MES, 2-(N-

morpholino)ethanesulfonic acid buffer; APS, ammonium persulfate; TEMED,

tetramethylethylenediamine; EtO, ethylene oxide; HA, hyaluronic acid; GM, glycidyl

methacrylate; MA, methacrylated.

Acknowledgements

This project was funded by the National Plan for Science, Technology and Innovation

(MAARIFAH) - King Abdulaziz City for Science and Technology, the Kingdom of Saudi

Arabia, award number (15-MED5025-03). The authors also acknowledge with thanks the

Science and Technology Unit at King Abdulaziz University for their financial and technical

support.

Received: ((will be filled in by the editorial staff))

Revised: ((will be filled in by the editorial staff))

Published online: ((will be filled in by the editorial staff))

References

[1] N. Bölgen, F. Plieva, I. Galaev, B. Mattiasson, E. Pişkin, "Cryogelation for preparation

of novel biodegradable tissue-engineering scaffolds", 2007, p. 1165.

[2] N. A. Peppas, J. Z. Hilt, A. Khademhosseini, R. Langer, Advanced Materials 2006, 18,

1345.

[3] B. V. Slaughter, S. S. Khurshid, O. Z. Fisher, A. Khademhosseini, N. A. Peppas,

Advanced Materials 2009, 21, 3307.

[4] S. A. Bencherif, J. A. Sheehan, J. O. Hollinger, L. M. Walker, K. Matyjaszewski, N. R.

Washburn, Journal of Biomedical Materials Research Part A: 2009, 90, 142.

15

- [5] S. Bencherif, O. Gsib, C. Egles, *J. Mol. Biol. Biotech* **2017**, *2*, 1.
- [6] S. Lin Gibson, S. Bencherif, J. M. Antonucci, R. L. Jones, F. Horkay, "Synthesis and characterization of poly (ethylene glycol) dimethacrylate hydrogels", in *Macromolecular symposia*, Wiley Online Library, 2005, p. 227/243.
- [7] C. Qi, J. Lin, L.-H. Fu, P. Huang, Chemical Society Reviews 2018, 47, 357.
- [8] M. E. Furth, A. Atala, M. E. Van Dyke, *Biomaterials* **2007**, *28*, 5068.
- [9] A. Memic, H. A. Alhadrami, M. A. Hussain, M. Aldhahri, F. Al Nowaiser, F. Al-Hazmi,
   R. Oklu, A. Khademhosseini, *Biomed. Mater.* 2015, 11, 014104.
- [10] H. J. Busscher, H. C. van der Mei, G. Subbiahdoss, P. C. Jutte, J. J. van den Dungen, S.
   A. Zaat, M. J. Schultz, D. W. Grainger, *Science translational medicine* 2012, 4, 153rv10.
- [11] W. L. Stoppel, J. C. White, S. D. Horava, A. C. Henry, S. C. Roberts, S. R. Bhatia, Journal of Biomedical Materials Research Part B: Applied Biomaterials 2014, 102, 877.
- [12] R. Galante, T. J. Pinto, R. Colaço, A. P. Serro, *Journal of Biomedical Materials Research Part B: Applied Biomaterials* **2018**, *106*, 2472.
- [13] W. A. Rutala, D. J. Weber, American Journal of Infection Control 2013, 41, S2.
- [14] E. M. Noah, J. Chen, X. Jiao, I. Heschel, N. Pallua, *Biomaterials* **2002**, *23*, 2855.
- [15] M. A. de Moraes, R. F. Weska, M. M. Beppu, *Journal of Biomedical Materials Research*Part B: Applied Biomaterials **2014**, 102, 869.
- [16] B. Li, J. Li, J. Xia, J. Kennedy, X. Yie, T. Liu, Carbohydrate Polymers 2011, 83, 44.
- [17] S. Lerouge, "Sterilization and cleaning of metallic biomaterials", in *Metals for Biomedical Devices*, Elsevier, 2019, p. 405.
- [18] Z. Dai, J. Ronholm, Y. Tian, B. Sethi, X. Cao, *J Tissue Eng* **2016**, *7*, 2041731416648810.
- [19] P. R. Marreco, P. d. L. Moreira, S. C. Genari, Â. M. Moraes, *Journal of Biomedical Materials Research Part B: Applied Biomaterials* **2004**, *71B*, 268.
- [20] C. E. Holy, C. Cheng, J. E. Davies, M. S. Shoichet, *Biomaterials* **2000**, *22*, 25.

- [21] N. Huebsch, M. Gilbert, K. E. Healy, *Journal of Biomedical Materials Research Part B: Applied Biomaterials* **2005**, *74B*, 440.
- [22] W. A. Rutala, D. J. Weber, 2008.
- [23] N. Haridas, M. Rosemary, Polymer degradation and stability 2019, 163, 220.
- [24] L. J. White, T. J. Keane, A. Smoulder, L. Zhang, A. A. Castleton, J. E. Reing, N. J. Turner, C. L. Dearth, S. F. Badylak, *Journal of Immunology and Regenerative Medicine* **2018**, *2*, 11.
- [25] P. Villard, M. Rezaeeyazdi, T. Colombani, K. Joshi Navare, D. Rana, A. Memic, S.A. Bencherif, *Advanced healthcare materials* **2019**, 1900679.
- [26] L. J. Eggermont, Z. J. Rogers, T. Colombani, A. Memic, S. A. Bencherif, *Trends Biotechnol.* **2019**.
- [27] A. Memic, T. Colombani, L. J. Eggermont, M. Rezaeeyazdi, J. Steingold, Z. J. Rogers,
   K. J. Navare, H. S. Mohammed, S. A. Bencherif, *Advanced Therapeutics* 2019, 2,
   1800114.
- [28] S. A. Bencherif, R. W. Sands, D. Bhatta, P. Arany, C. S. Verbeke, D. A. Edwards, D. J. Mooney, *Proceedings of the National Academy of Sciences* 2012, 109, 19590.
- [29] A. Béduer, T. Braschler, O. Peric, G. E. Fantner, S. Mosser, P. C. Fraering, S. Benchérif,
   D. J. Mooney, P. Renaud, *Advanced Healthcare Materials* 2015, 4, 301.
- [30] A. Memic, T. Colombani, L. J. Eggermont, M. Rezaeeyazdi, J. Steingold, Z. J. Rogers,K. J. Navare, H. S. Mohammed, S. A. Bencherif, *Advanced Therapeutics* 2019, 1800114.
- [31] T. Y. Shih, S. O. Blacklow, A. W. Li, B. R. Freedman, S. Bencherif, S. T. Koshy, M. C. Darnell, D. J. Mooney, *Advanced healthcare materials* **2018**, *7*, 1701469.
- [32] M. Rezaeeyazdi, T. Colombani, A. Memic, S. A. Bencherif, *Materials* **2018**, *11*, 1374.
- [33] S. A. Bencherif, A. Srinivasan, F. Horkay, J. O. Hollinger, K. Matyjaszewski, N. R. Washburn, *Biomaterials* 2008, 29, 1739.

- [34] S. A. Bencherif, R. W. Sands, O. A. Ali, W. A. Li, S. A. Lewin, T. M. Braschler, T.-Y.
  S. Shih, C. S. Verbeke, D. Bhatta, G. Dranoff, D. J. Mooney, *Nature communications*2015, 6, 7556.
- [35] S. A. Bencherif, R. W. Sands, D. Bhatta, P. Arany, C. S. Verbeke, D. A. Edwards, D. J. Mooney, Proceedings of the National Academy of Sciences of the United States of America 2012, 109, 19590.
- [36] M.-E. Han, S.-H. Kim, H. D. Kim, H.-G. Yim, S. A. Bencherif, T.-I. Kim, N. S. Hwang, International journal of biological macromolecules **2016**, *93*, 1410.
- [37] J. Kim, S. A. Bencherif, W. A. Li, D. J. Mooney, *Macromolecular rapid* communications **2014**, *35*, 1578.
- [38] A. San Juan, A. Montembault, D. Gillet, J. Say, S. Rouif, T. Bouet, I. Royaud, L. David, "Degradation of chitosan-based materials after different sterilization treatments", in *IOP Conference Series: Materials Science and Engineering*, IOP Publishing, 2012, p. 31/012007.
- [39] C. Jarry, C. Chaput, A. Chenite, M. A. Renaud, M. Buschmann, J. C. Leroux, *Journal of Biomedical Materials Research* **2001**, *58*, 127.
- [40] Y. Lee, D. Balikov, J. Lee, S. Lee, S. Lee, J. Lee, K. Park, H.-J. Sung, *International journal of molecular sciences* **2017**, *18*, 1705.
- [41] S. A. Bencherif, N. R. Washburn, K. Matyjaszewski, *Biomacromolecules* **2009**, *10*, 2499.
- [42] S. A. Bencherif, A. Srinivasan, J. A. Sheehan, L. M. Walker, C. Gayathri, R. Gil, J. O. Hollinger, K. Matyjaszewski, N. R. Washburn, *Acta biomaterialia* **2009**, *5*, 1872.
- [43] J. D. Kretlow, L. Klouda, A. G. Mikos, Advanced Drug Delivery Reviews 2007, 59, 263.
- [44] T. Takei, S. Danjo, S. Sakoguchi, S. Tanaka, T. Yoshinaga, H. Nishimata, M. Yoshida, *Journal of bioscience and bioengineering* **2018**, *125*, 490.

- [45] M. Yavari-Gohar, K. Kabiri, M. Zohuriaan-Mehr, S. Hashemi, *Journal of polymer research* **2010**, *17*, 151.
- [46] M. Liu, X. Zeng, C. Ma, H. Yi, Z. Ali, X. Mou, S. Li, Y. Deng, N. He, **2017**, *5*, 17014.
- [47] U. Lampe, M. Maier, J. E. Klee, H. Ritter, *Polymer International* **2016**, *65*, 1142.
- [48] H. Tan, K. G. Marra, *Materials* **2010**, *3*, 1746.
- [49] S. Mitragotri, J. Lahann, *Nature materials* **2009**, *8*, 15.
- [50] S. J. Hollister, *Nature materials* **2005**, *4*, 518.
- [51] L. Cai, R. E. Dewi, S. C. Heilshorn, Advanced functional materials 2015, 25, 1344.
- [52] A. K. Gaharwar, N. A. Peppas, A. Khademhosseini, *Biotechnology and bioengineering* **2014**, *111*, 441.
- [53] N. Faramarzi, I. K. Yazdi, M. Nabavinia, A. Gemma, A. Fanelli, A. Caizzone, L. M. Ptaszek, I. Sinha, A. Khademhosseini, J. N. Ruskin, *Advanced healthcare materials* 2018, 7, 1701347.
- [54] D. Howard, L. D. Buttery, K. M. Shakesheff, S. J. Roberts, *Journal of anatomy* **2008**, *213*, 66.
- [55] L. G. Griffith, G. Naughton, Science 2002, 295, 1009.
- [56] F. Wang, L. A. Garza, S. Kang, J. Varani, J. S. Orringer, G. J. Fisher, J. J. Voorhees, Archives of dermatology 2007, 143, 155.
- [57] C. Liying, J. Kai, S. Ting-Yu, H. Anthony, G. Giorgio, M. D. J., O. D. P., N. C. S., Tissue Engineering Part A 2017, 23, 243.

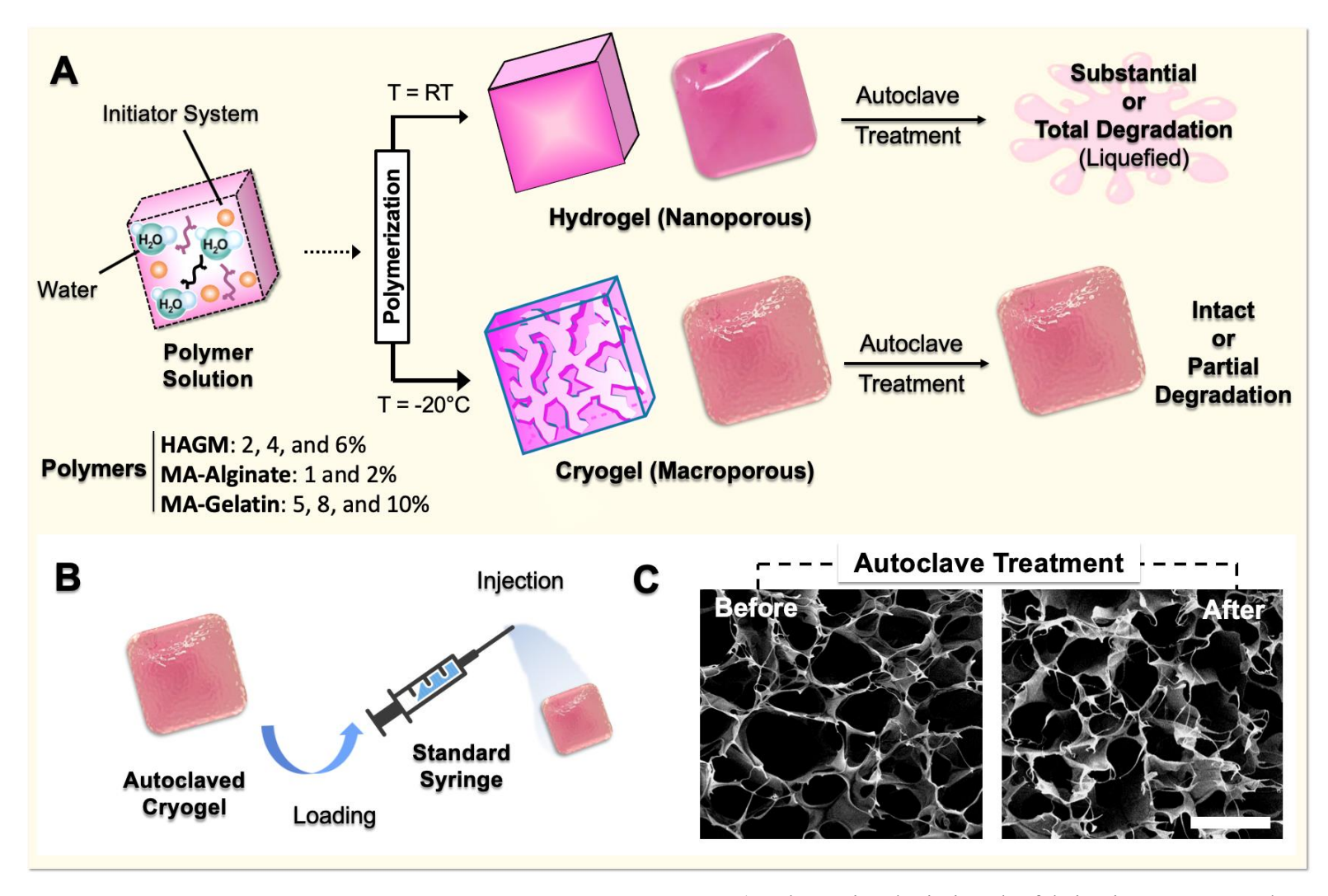
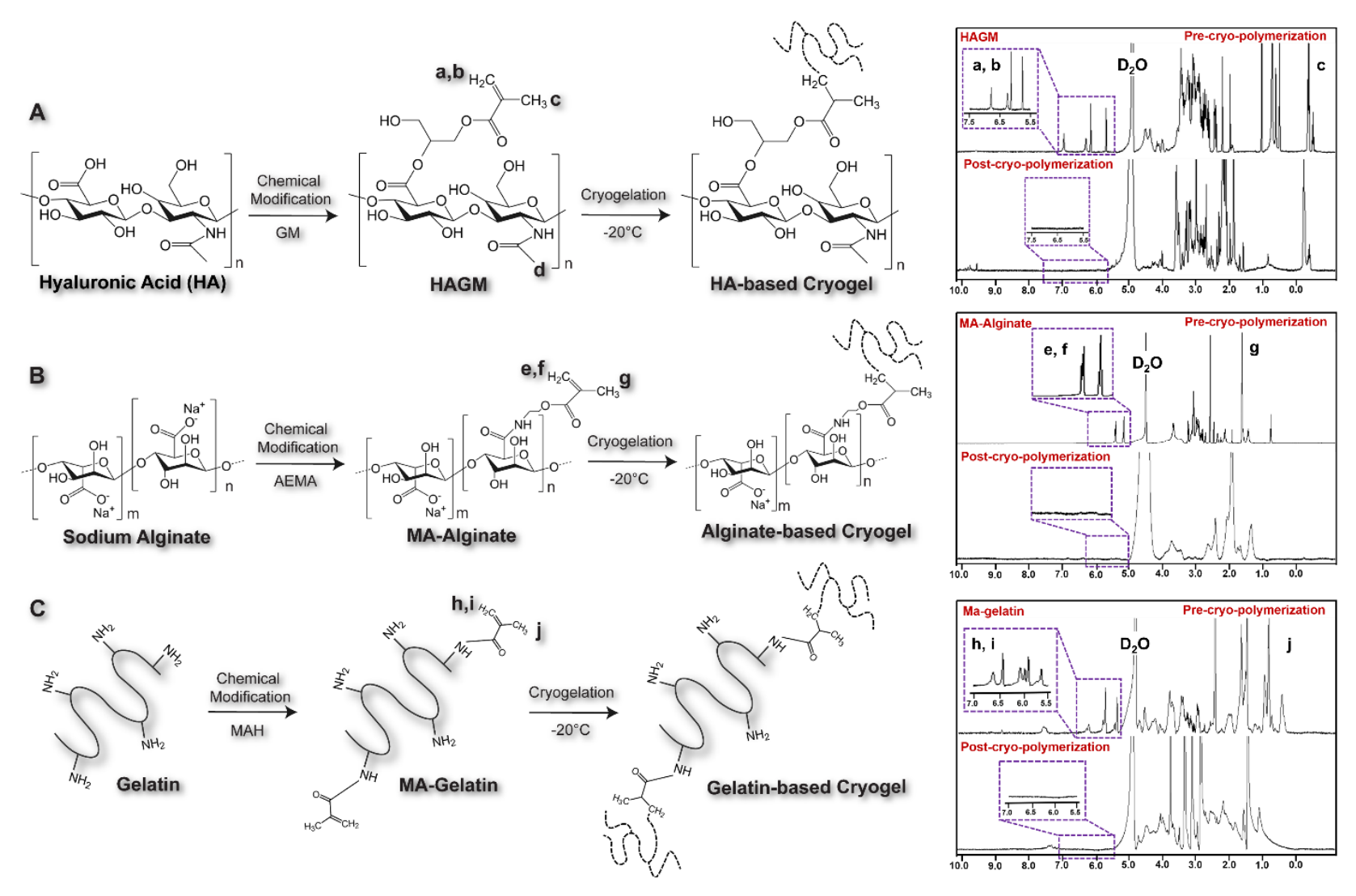


Figure 1. Engineering injectable and autoclavable cryogel scaffolds. A) Schematics depicting the fabrication process and autoclave treatment of hydrogels and cryogels at various polymer concentrations across three biopolymers: methacrylated hyaluronic acid (HAGM), alginate (MA-Alginate), and gelatin (MA-Gelatin). B) Photographs depicting shape-memory properties of autoclaved cryogels (colored in pink for visualization) before and after syringe injection. C) SEM images of a 4% w/v HAGM cryogel pre- and post-autoclave treatment. Scale bare =  $100 \, \mu m$ .



**Figure 2**. Chemical modification and characterization of biopolymers and their subsequent cryogelation. Schematics describing the methacrylation and successive cryopolymerization (left) and <sup>1</sup>H NMR spectra (right) of **A**) HAGM, **B**) MA-Alginate, and **C**) MA-Gelatin pre- and post-crosslinking. The vinylic peaks (between 5.5 and 7.0 ppm) disappeared after cryopolymerization at -20 °C across the three investigated biopolymers (4% HAGM, 2% MA-alginate, and 10% MA-Gelatin).

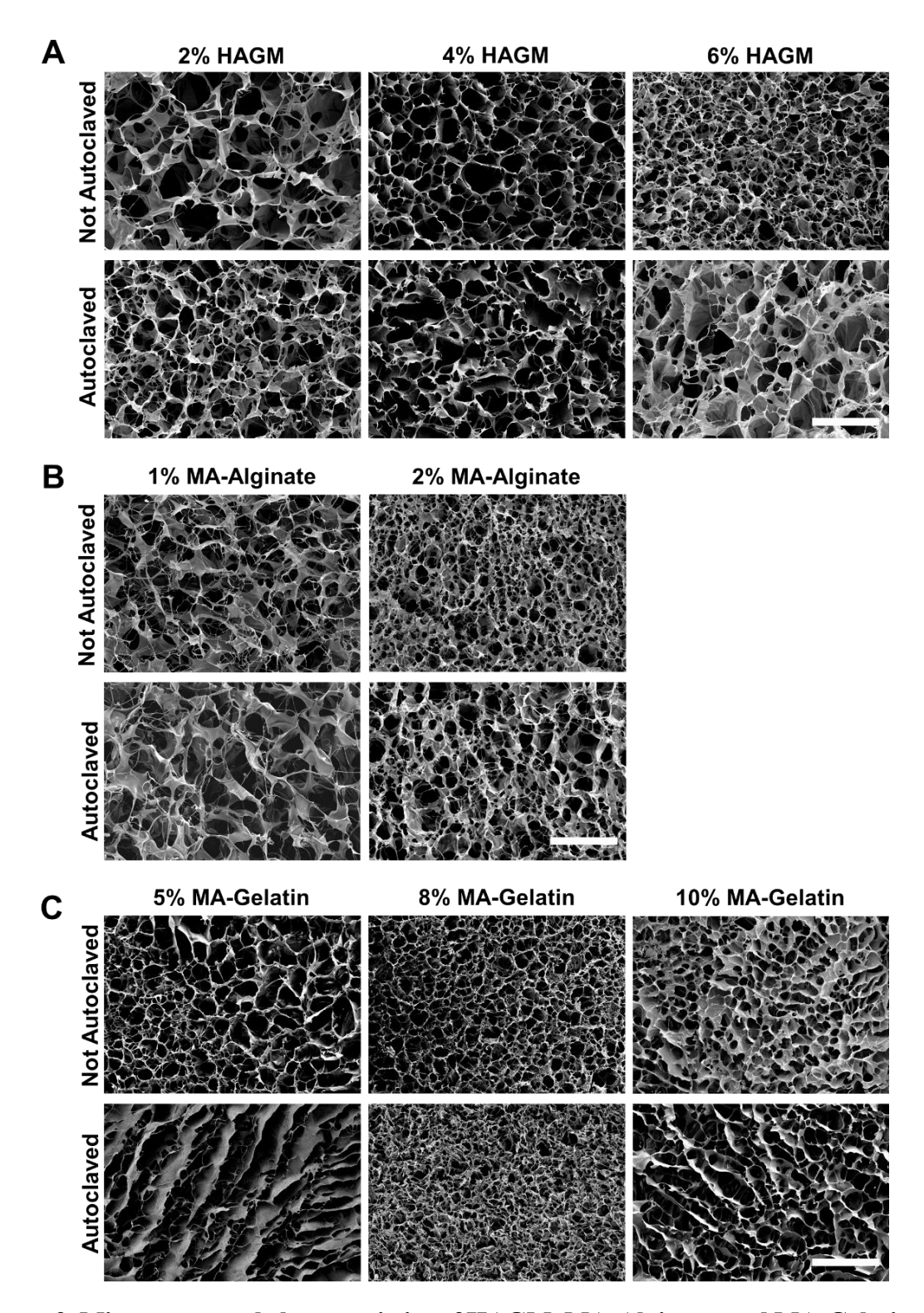


Figure 3. Microstructural characteristics of HAGM, MA-Alginate, and MA-Gelatin cryogels. SEM images of (A) HAGM, (B) MA-Alginate, and (C) MA-Gelatin cryogels formulated at various polymer concentrations pre- and post-autoclave treatment. Scale bar =  $100 \mu m$ .

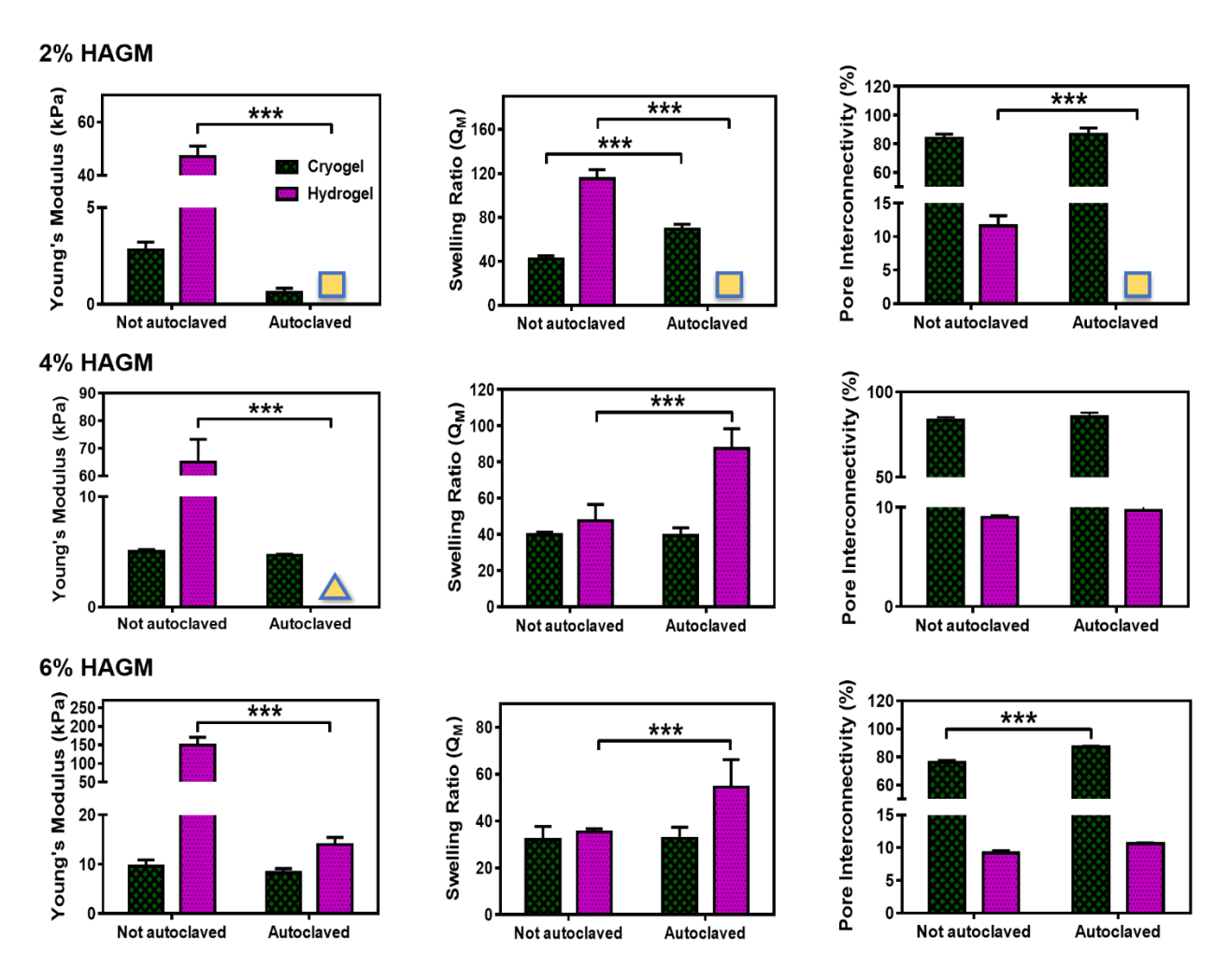


Figure 4. Physical properties of HA-based hydrogels and cryogels. Change in young's modulus, swelling ratio, and pore interconnectivity of HAGM cryogels and hydrogels with different concentration before and after autoclave sterilization. The squares (•) denote that no data are available as a result of complete gel degradation following autoclave sterilization. The triangle ( $\triangle$ ) denotes substantial gel degradation precluding mechanical characterization. Values represent mean and SD (n = 5). Data were analyzed using two-way ANOVA and Bonferroni post-test (compared to non-autoclaved conditions), \*\*\*p< 0.001.

#### 1% MA-Alginate Pore Interconnectivity (%) Young's Modulus (kPa) \*\*\* \*\*\* \*\*\* Swelling Ratio (Q<sub>M</sub>) Cryogel Hydrogel Not autoclaved Not autoclaved Autoclaved Not autoclaved Autoclaved Autoclaved 2% MA-Alginate Pore Interconnectivity (%) Young's Modulus (kPa) \*\*\* \*\*\* Swelling Ratio (Q<sub>M</sub>) \*\*\* 100-80-60 I Not autoclaved Autoclaved Not autoclaved Autoclaved Not autoclaved

Figure 5. Physical properties of Alginate-based hydrogels and cryogels. Change in young's modulus, swelling ratio, and pore interconnectivity of MA-Alginate cryogels and hydrogels with different concentration before and after autoclave sterilization. The squares ( $\bullet$ ) denote that no data are available as a result of complete gel degradation following autoclave sterilization. Values represent mean and SD (n = 5). Data were analyzed using two-way ANOVA and Bonferroni posttest (compared to non-autoclaved conditions), \*\*\*p< 0.001.

#### 5% MA-Gelatin Pore Interconnectivity (%) Young's Modulus (kPa) Swelling Ratio (Q<sub>M</sub>) Cryogel Hydrogel Not autoclaved Autoclaved Not autoclaved . Autoclaved Not autoclaved Autoclaved 8% MA-Gelatin Pore Interconnectivity (%) Young's Modulus (kPa) \*\*\* Swelling Ratio (Q<sub>M</sub>) 80-20. Not autoclaved Autoclaved Not autoclaved Autoclaved Not autoclaved Autoclaved 10% MA-Gelatin Young's Modulus (kPa) \*\*\* Swelling Ratio (Q<sub>M</sub>) \*\*\* 80. 100 20 **T** Not autoclaved Autoclaved Not autoclaved Autoclaved Not autoclaved Autoclaved

**Figure 6. Physical properties of Gelatin-based hydrogels and cryogels.** Change in young's modulus, swelling ratio, and pore interconnectivity of MA-Gelatin cryogels and hydrogels with different concentration before and after autoclave sterilization. The disks (O) denote that no data are available as no hydrogel was obtained at a low polymer concentration. The squares ( $\bullet$ ) denote that no data are available as a result of complete gel degradation following autoclave sterilization. Values represent mean and SD (n = 5). Data were analyzed using two-way ANOVA and Bonferroni post-test (compared to non-autoclaved conditions), \*p< 0.05, \*\*p< 0.01, and \*\*\*p< 0.001.

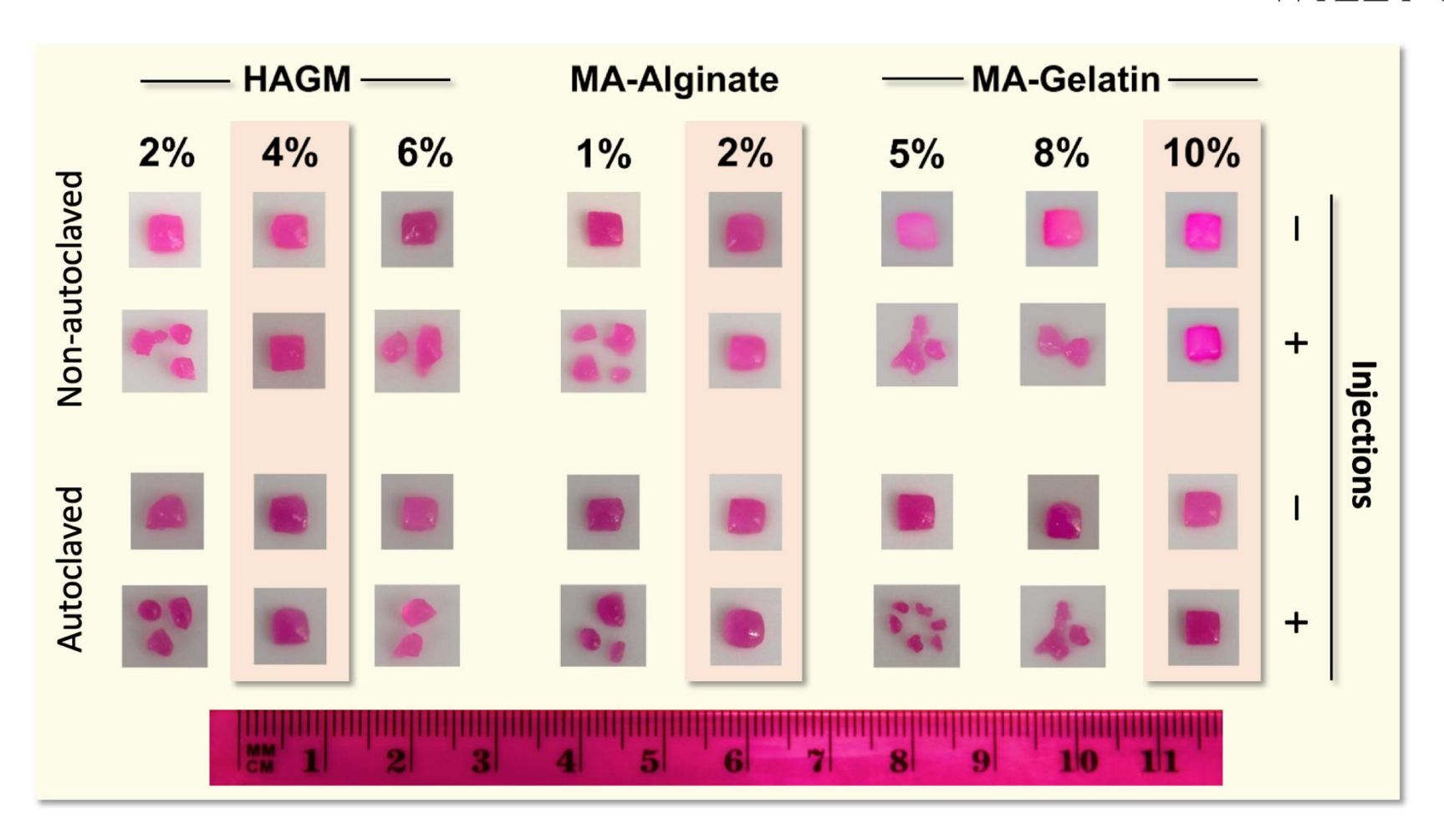


**Figure 7. Syringeability and injectability of non-autoclaved and autoclaved cryogels.** Photographs showing syringe injected cryogels made from three different rhodamine-labeled biopolymers at various polymer concentrations (HAGM: 2-6 % w/v, MA-Alginate: 1-2 % w/v, and MA-Gelatin: 5-10 % w/v). These square-shaped cryogels (dimensions: 4 mm x 4 mm x 1 mm) were first subjected to autoclave sterilization and subsequently syringe injected. All cryogel samples were all pushed through 16G hypodermic needles and tested for their syringeability and injectability.

### **Table of Contents**

Effect of polymer concentration on the properties of autoclavable cryogels made from naturally-derived polymer precursors is reported for the first time. The structural and physical properties of autoclaved cryogels are thoroughly investigated. The results show that at optimal polymer concentrations, autoclave sterilization does not substantially alter the microarchitectural and physical characteristics of shape-memory cryogels, including their distinctive syringe injectability.

Keywords: Autoclave Sterilization, Biopolymers, Physical Properties, Cryogels, Biomedical Applications

Authors: Adnan Memic, Mahboobeh Rezaeeyazdi, Pierre Villard, Zachary J. Rogers, Tuerdimaimaiti Abudula, Thibault Colombani, Sidi A. Bencherif\*

Title: Effect of Polymer Concentration on Autoclaved Cryogel Properties

